



**COMSOL
CONFERENCE**
2019 BANGALORE

Numerical Simulation of Melt Hydrodynamics in Laser Micro-Processing using COMSOL Multiphysics®

Shashank Sharma
Prof. J. Ramkumar
Prof. S. A. Ramakrishna

Dept. of Mechanical Engineering, IIT Kanpur
Dept. of Physics, IIT Kanpur

Laser ~~Does~~ Manufacturing Matters?

 70% Manufacturing share of global Trade

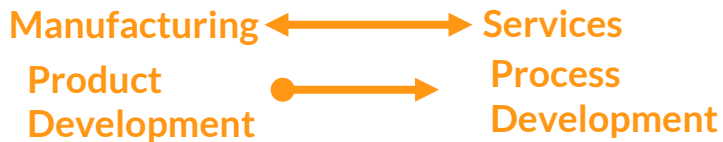
 16 % Manufacturing share in Global GDP

 \$726 Billions Trade surplus of advance economies in innovative goods

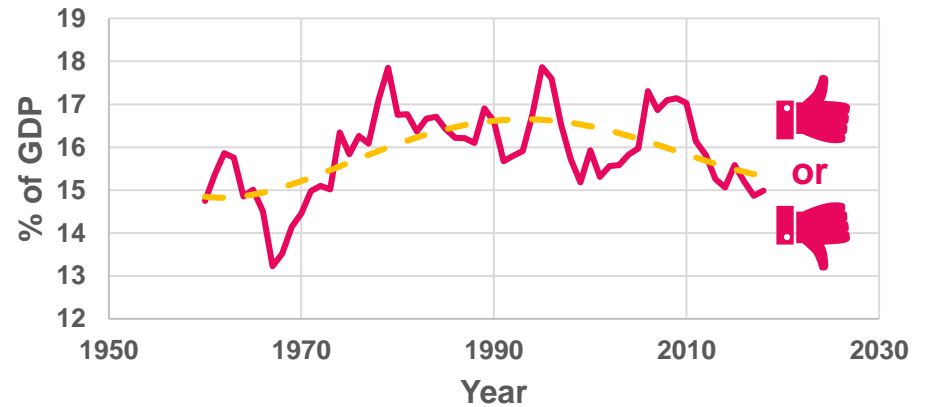
 Laser processing market to grow from USD 6.40 Billion in 2015 to USD 9.75 Billion by 2022, at a CAGR of 6.13% from 2016 to 2022

 The laser processing market in APAC is expected to hold the largest share during the forecast period. India is expected to grow at 19% CAGR to €1 billion by 2020.

Manufacturing is not Monolithic



Manufacturing, value added (% of GDP, India)



Source: World Bank (OECD National Accounts data files)

 < 17 % Manufacturing share in Indian GDP (3rd largest Economy)

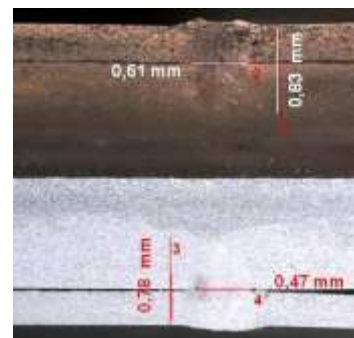
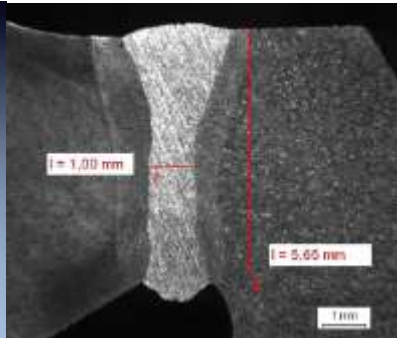
 India's share of global manufacturing value added is ~2%

 \$138 Billions Trade deficit

Target: 25 % Manufacturing share in Indian GDP (Make in India)



Pictorial representation of Laser processing Applications in Auto industry



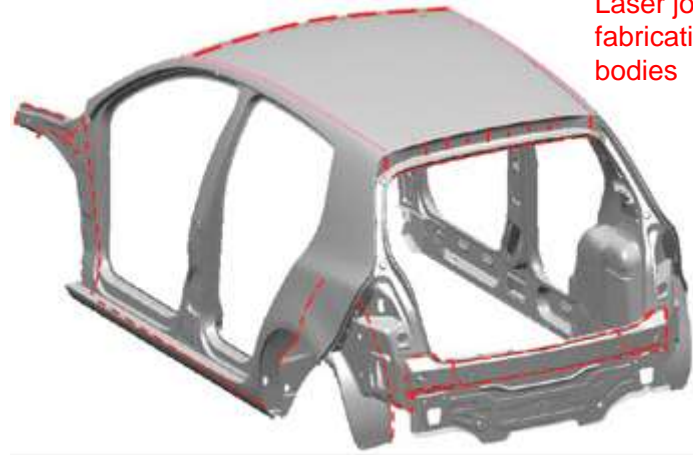
Laser Welding of Bus-bar, Cu-Cu; Al-Al, 3 mm-1 mm

Laser Welding of Differential gears, case hardened steel, Laser power 4kW; image source: https://automotivemanufacturingsolutions.com/wp-content/uploads/2013/12/AMSI_2013_Andrey_Andreev.pdf



Laser Welded Solenoid used in cars

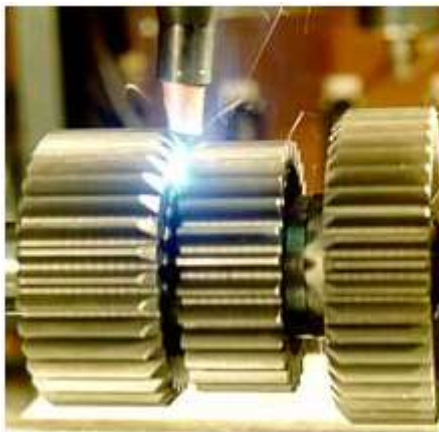
Image source: <https://www.twi-global.com/technical->



Laser joining for fabricating car bodies

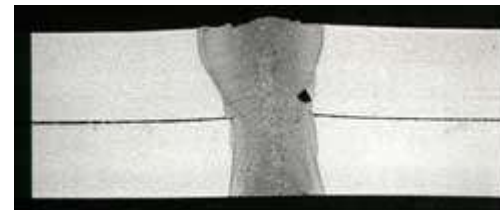


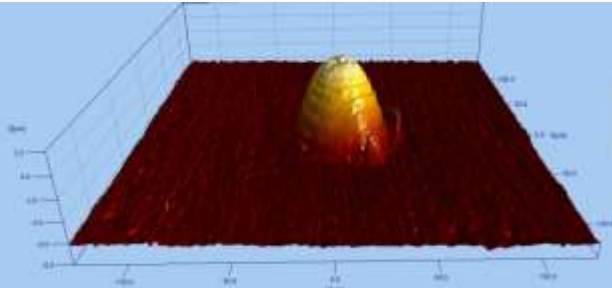
This axle component found on a Mercedes C Class sedan was laser hybrid welded at 177 IPM (4.5 m/min.) with a wire feed rate of 235 IPM (6.0 m/min.) Image source: <https://www.thefabricator.com/article/laserwelding/a-look-at-laser-hybrid-welding-in-the-automotive-industry>.



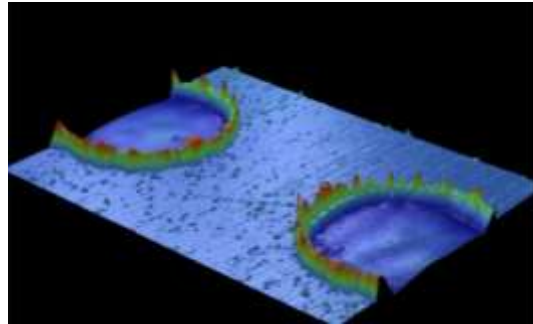
CO2 Laser welding of gear component

Lap joint in 1.6mm thick 5754 aluminum alloy sheet welded at 5m/min with CO 2 laser

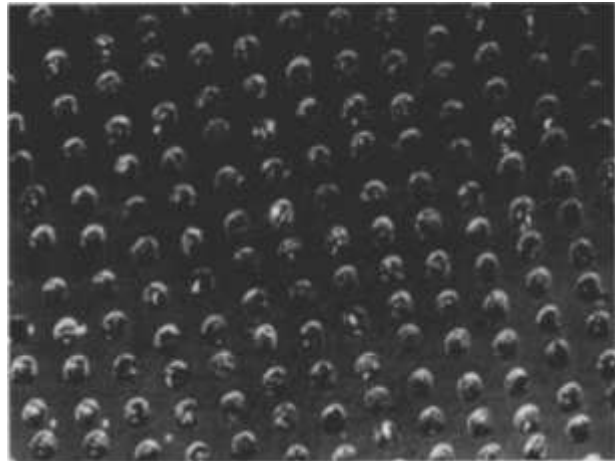




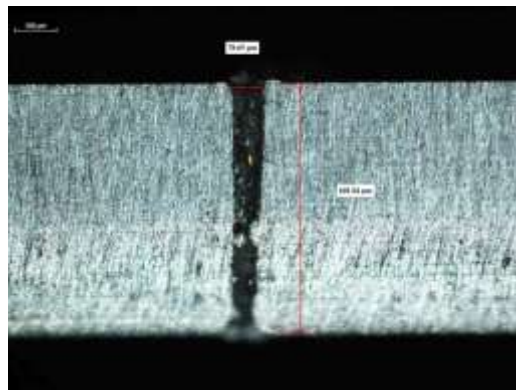
50 μm convex dome in steel



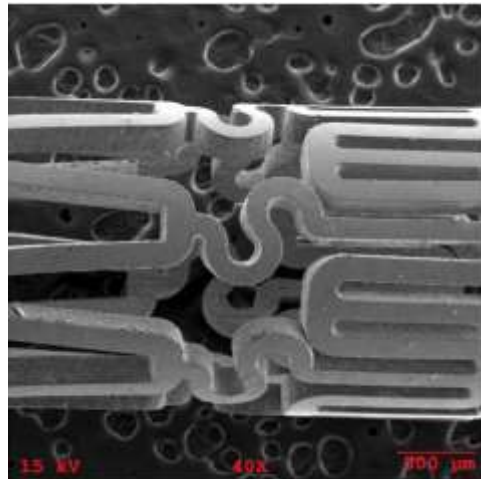
100 μm holes in steel



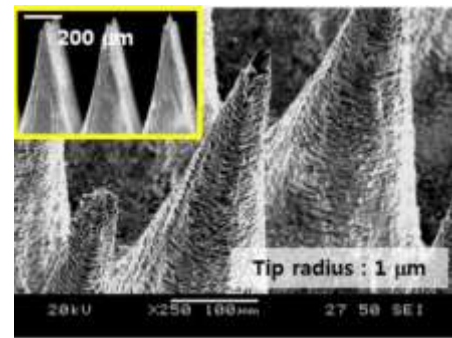
LST regular micro-surface structure in the form of micro-dimples [Etsion et. al.]



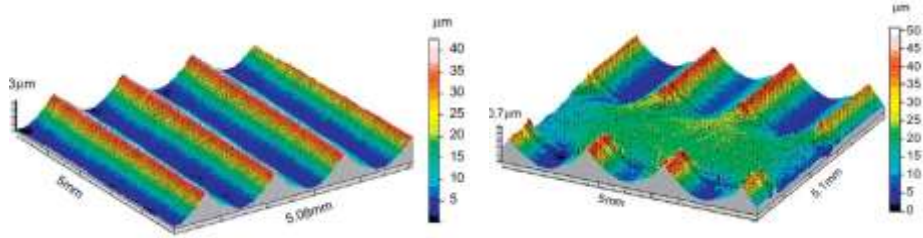
$\sim 80 \mu\text{m}$ hole drilled through a 600 μm Ti sheet



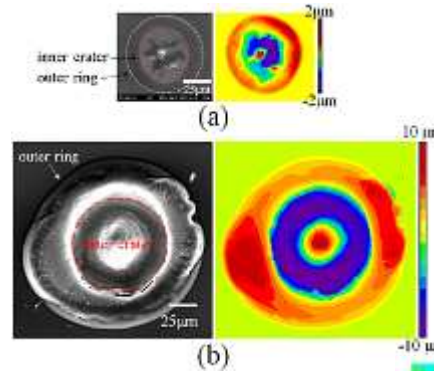
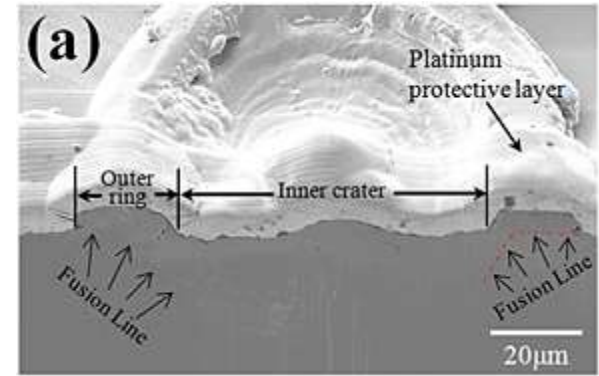
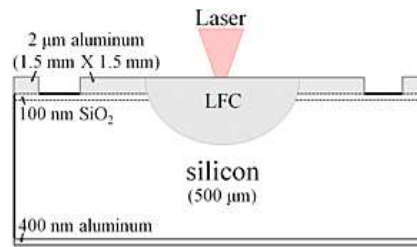
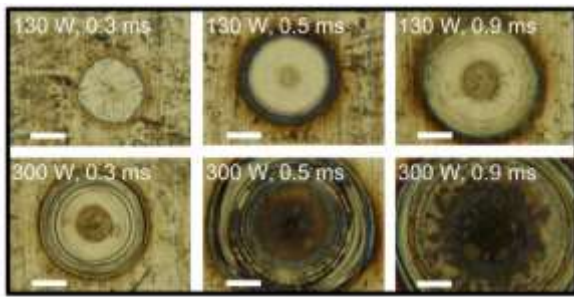
Fiber Laser cut nitinol stent [Baumeister et al.]



fabricated micro pin array on tungsten [Park et. al.]

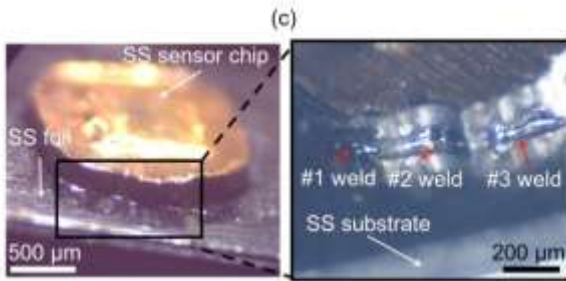


Laser micro polishing

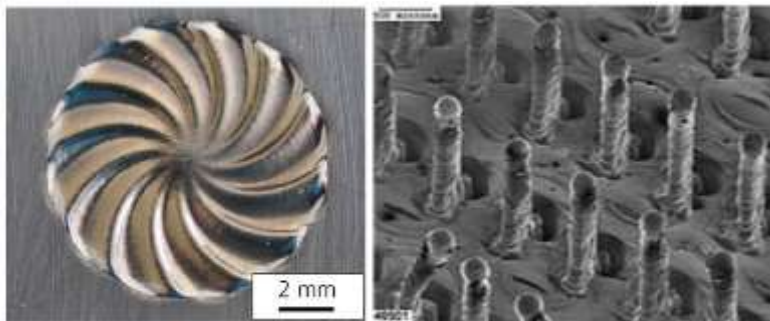
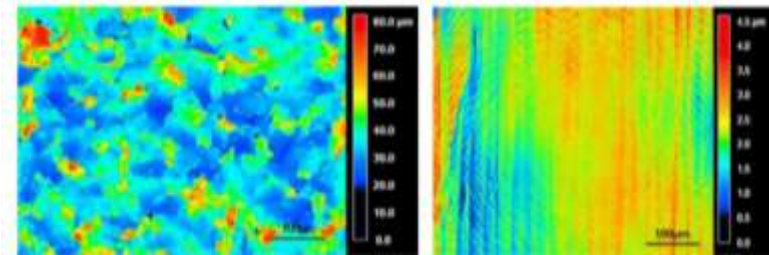


laser-fired contact processed with 260 W laser power, 30 μs pulse length and 70 μm dia. [Raghavan et. al.]

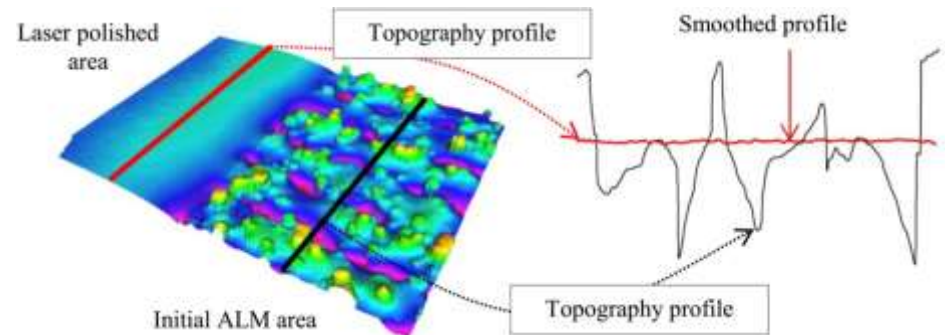
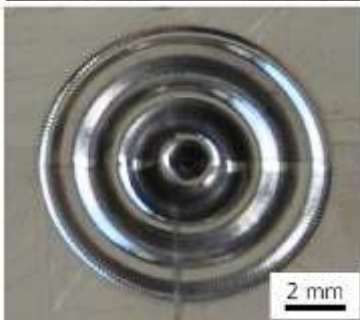
A fabricated sensor welded on SS foil [Chen et. al.]



Laser polishing of additive manufactured Ti alloys. [C. Ma et. al.]



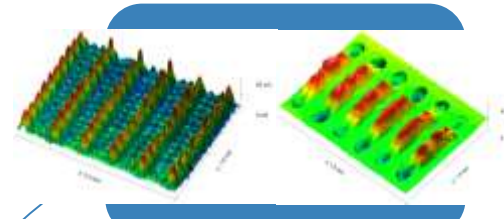
Laser sculpting by re-melting. [Temmler M. Et. al.]



[Benoit Rosa et. al.]

Research Spectrum of Laser micro-sacle Processing of metals

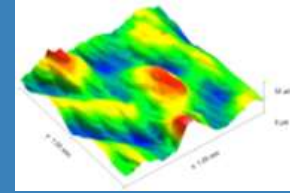
Laser Processing Applications



Large area surface structuring of SS 304 substrate using melt hydrodynamics



~80 μm hole drilled through a 600 μm Ti sheet



Surface asperities homogenization after single laser raster scanning on SS 304



Optical Micrograph of keyhole mode and conduction mode laser μ -welding of SS 304

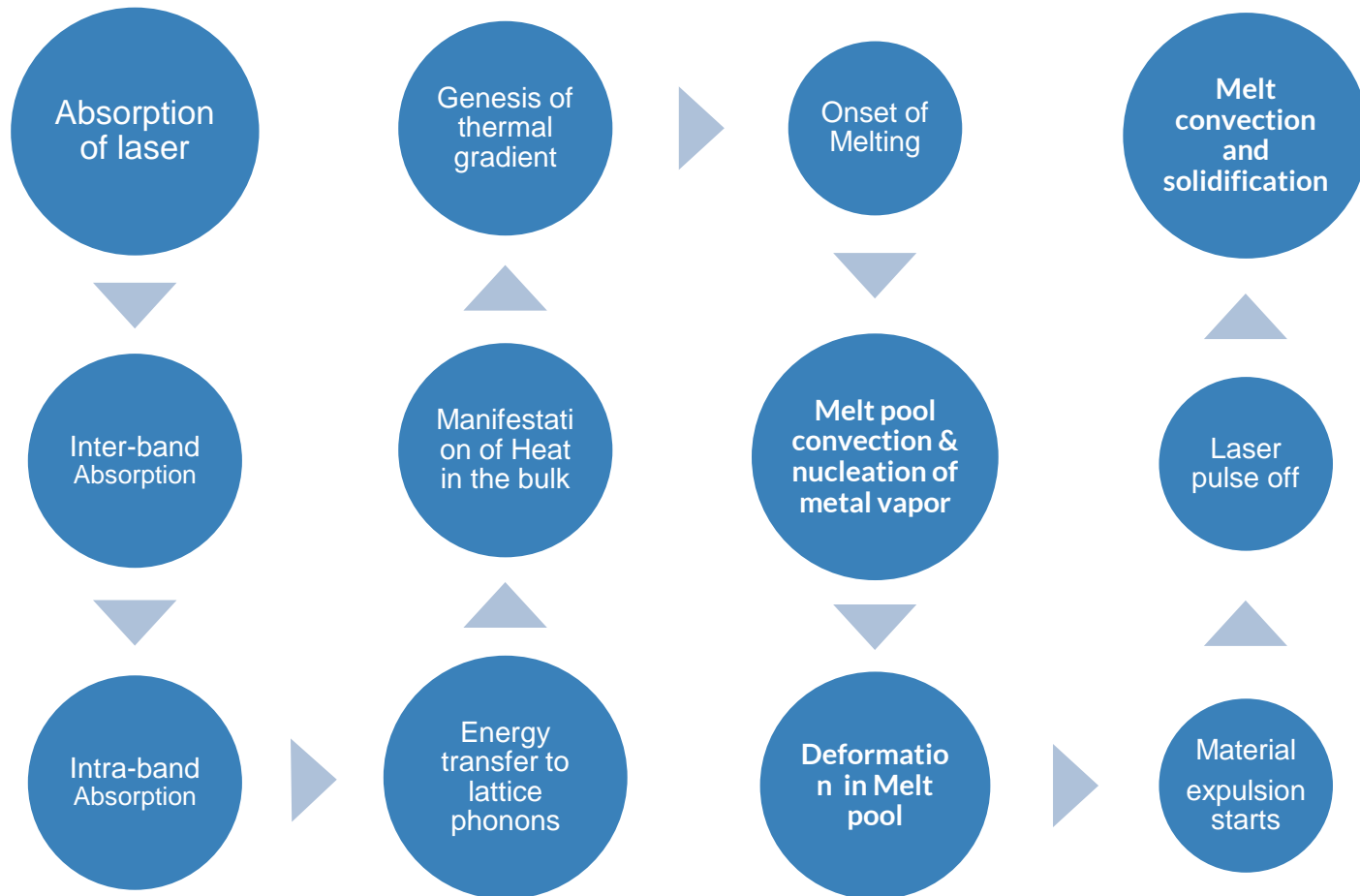
Limitations of Laser Material processing

- Melt shadowing effect in Laser-drilling.
- Melt-induced recast layer and surface roughness in laser drilling.
- Humping phenomenon in micro laser welding, for micro joining.
- Porosity, Waviness and melt ripples in welded structure.
- Surface over melting in micro polishing and structuring of metals.



Understanding Melt Pool Convection: Water waves analogy

Laser-matter interaction



Key parameters

1

Laser intensity

The order of intensity dictates the mechanism of interaction.

Low intensity- melting.
High intensity- melting and vaporization.

2

Pulse duration

Influences the thermal penetration which in turn affects melt depth, heat affected zone area.

3

Thermo-capillary forces

With the genesis of thermal gradients, marangoni force starts to act on melt surface, producing perturbation over a thin melt layer.

4

Evaporative Heat flux

With vaporization, cooling of subsequent melted surface resulting in temperature dependent melt dynamics.

5

Recoil Pressure

Normal pressure by receding vapor on melt surface, responsible of melt layer deformation.

6

Surface Tension

Another normal force which balances recoil pressure during heating and responsible for retraction of melt during cooling.

Numerical Simulation

Laser Absorption

- Multiple reflections of laser beam is ignored.
- Fresnel Absorption implemented, where θ_i is angle of incidence which depends upon surface curvature.

$$A_p = 1 - \frac{(n^2 + k^2)\cos^2(\theta_i) - 2n\cos(\theta_i) + 1}{(n^2 + k^2)\cos^2(\theta_i) + 2n\cos(\theta_i) + 1}$$

$$A_s = 1 - \frac{(n^2 + k^2)\cos^2(\theta_i) - 2n\cos(\theta_i) + \cos^2(\theta_i)}{(n^2 + k^2)\cos^2(\theta_i) + 2n\cos(\theta_i) + \cos^2(\theta_i)}$$

$$\alpha = \frac{A_p + A_s}{2}$$

Laser Heating

- Heat Transfer module, with temperature dependent thermo-physical properties i.e. $\rho(T)$, $\kappa(T)$, $C_p(T)$.
- Phase change.
- Radiation loss.
- Ambient heat transfer.
- Evaporative heat loss.

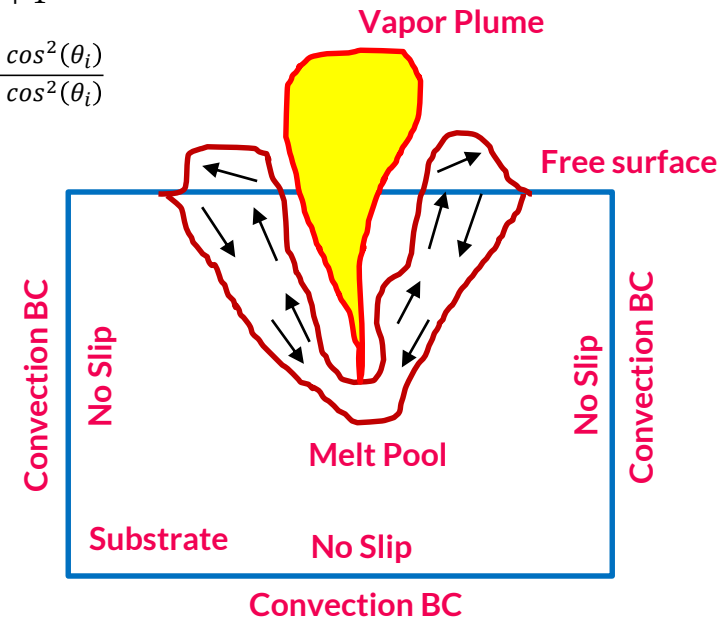
Melt Pool Convection

- Laminar Flow module, with temperature dependent thermo-physical properties i.e. $\rho(T)$, $\mu(T)$, $\sigma(T)$.
- Natural Convection.
- Marangoni Convection (temperature gradient & **concentration** gradient).
- Vaporization Induced Recoil pressure
- Free Surface (effects of surface tension).

Free Surface Handling :
ALE/
Level-Set/
Phase Field

Adaptability with
changing
Laser
processing
operation

Realistic Values
of Thermo-
physical
parameters



Assumptions

- Flow of liquid metal is incompressible Newtonian laminar flow.
- Metallic vapor is regarded as ideal gas and transparent to laser beam.
- Plasma formation and multiple reflections are not taken in account.
- All thermo-physical properties are function of temperature.

Numerical Simulation

Heat transfer + Laminar Flow

Governing Equations

$$\rho C_p^{eq} \left[\frac{\partial T}{\partial t} + \vec{\nabla} \cdot (\vec{u} T) \right] = \vec{\nabla} \cdot (k \vec{\nabla} T)$$

$$\rho \left(\frac{\partial \vec{u}}{\partial t} + \vec{u} \cdot (\vec{\nabla} \cdot \vec{u}) \right)$$

$$= \vec{\nabla} \cdot \left[-pI + \mu (\vec{\nabla} \vec{u} + (\vec{\nabla} \cdot \vec{u})^T) \right] + \rho \vec{g} - \rho_i \beta (T - T_m) \vec{g}$$

$$\vec{\nabla} \cdot \vec{u} = 0$$

Boundary Conditions

$$Q_{laser} = 2.5 \cos(\theta) \alpha(\theta) f(t) \frac{P}{\pi r_0^2} \left[\frac{-((x-vel \cdot t)^2 - (y)^2)}{r_0^2} \right] \delta(\phi)$$

$$Q_{losses} = -q_{evap} - h[T - T_{amb}] - \epsilon \sigma [T^4 - T_{amb}^4] \delta(\phi)$$

$$q_{evap} = M_v \times L_v$$

$$M_v = \sqrt{\frac{m}{2\pi k_b T_s}} \times P_{sat}(T_s) \times (1 - \beta_r)$$

$$P_{sat}(T_s) = P_{atm} \times \exp\left(\frac{M_a L_v}{R} \left(\frac{1}{T_v} - \frac{1}{T_s}\right)\right)$$

$$P_{recoil} = \begin{cases} P_{amb}, & 0 \leq T_s < T_c \\ \frac{1+\beta_r}{2} \times P_{sat}(T_s), & T_s \geq T_c \end{cases} \delta(\phi)$$

$$\vec{F} = -(P_{recoil} - P_{amb})\vec{n} + \sigma(\vec{\nabla}_s \cdot \vec{n})\vec{n} - \vec{\nabla}_s \sigma$$

Mathematics Module : Moving Interface

ALE

$$n_i \cdot ((P_1 - P_2)I - \mu_1(\nabla u_1 - (\nabla u_1)^T) + \mu_2(\nabla u_2 - (\nabla u_2)^T)) = \sigma(\nabla_s \cdot n_i)n_i - \nabla_s \sigma$$

$$\mu_1 \gg \mu_2, \text{ pressure jump at interface } P_2 - P_1 = P_{recoil}$$

$$n_i \cdot (\mu(\nabla u - (\nabla u)^T)) = -P_{recoil}n_i + \sigma(\nabla_s \cdot n_i)n_i - \nabla_s \sigma$$

$$\sigma = \sigma_m - \gamma_{pm}(T - T_m) - R_g T \Gamma_s \ln(1 + k_1 a_i e^{-\frac{\Delta H_o}{R_g T}})$$

$$\frac{d\sigma}{dT} = -\gamma_{pm} - R_g T \Gamma_s \ln(1 + K a_i) - \frac{K a_i}{1 + K a_i} \frac{\Gamma_s \Delta H_o}{T}$$

$$\frac{\partial \vec{X}}{\partial t} \cdot \vec{n} = \vec{u}$$

Mesh Smoothing Type

- Hyperelastic
- Yeoh
- Mesh size must be comparable to deformation at each time step

Fully coupled solver

Level-set

$$\frac{\partial \phi}{\partial t} + \vec{u} \cdot \vec{\nabla} \phi + \gamma \vec{\nabla} \cdot \left[\phi(1 - \phi) \frac{\vec{\nabla} \phi}{|\vec{\nabla} \phi|} - \epsilon \vec{\nabla} \phi \right] = 0$$

$$S_{cont} = \delta(\phi) M_v \left(\frac{\rho_l - \rho}{\rho^2} \right)$$

$$S_{ls} = \delta(\phi) M_v \left(\frac{\phi}{\rho_l} + \frac{1 - \phi}{\rho_v} \right)$$

Alternative to ALE

- Extreme Topological Changes
- Suitable for melt expulsion regime
- Interface aberration occurs during vaporization dominant regime with realistic values of surface tension

Alternative to ALE

- Extreme Topological Changes
- Suitable for vaporization dominant regime with realistic values of surface tension

Phase-field

$$\frac{\partial \phi}{\partial t} + u \cdot \nabla \phi = \nabla \cdot \frac{\gamma \lambda}{\epsilon^2} \nabla \psi$$

$$\psi = -\nabla \cdot \epsilon^2 \nabla \phi + (\phi^2 - 1)\phi$$

$$\delta = 6|\phi(1 - \phi)| |\nabla \phi|$$

$$\nabla \cdot \vec{u} = \delta * (M_v * \left(\frac{\rho_l - \rho}{\rho^2} \right))$$

$$\frac{\partial \phi}{\partial t} + u \cdot \nabla \phi - \delta * (M_v * \left(\frac{\rho_l - \rho}{\rho^2} \right)) = \nabla \cdot \frac{\gamma \lambda}{\epsilon^2} \nabla \psi$$

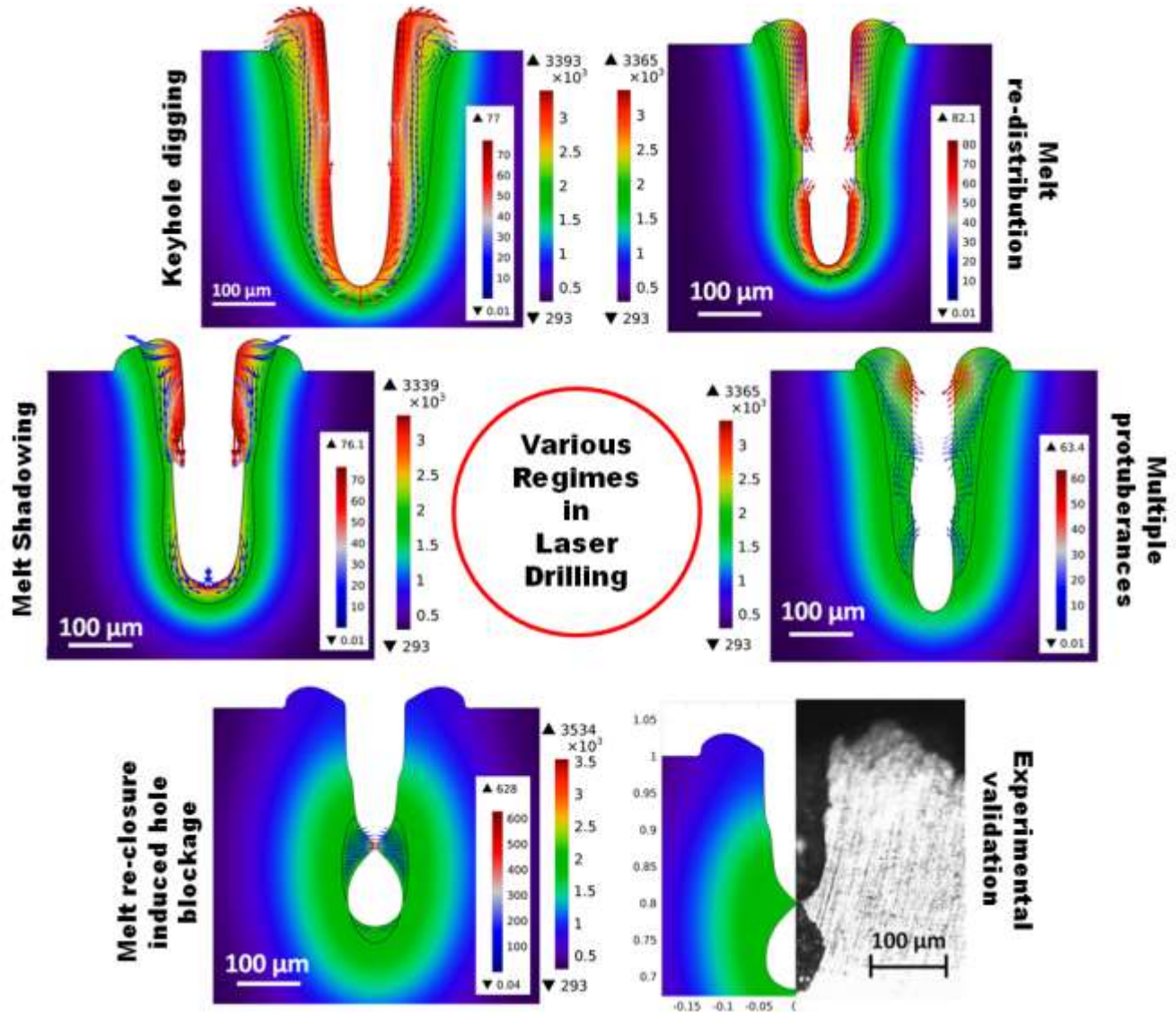
Meshing

- Interface thickness
- Mesh size must resolve moving interface

Segregated solver $\delta(\phi) \rightarrow T \rightarrow U$

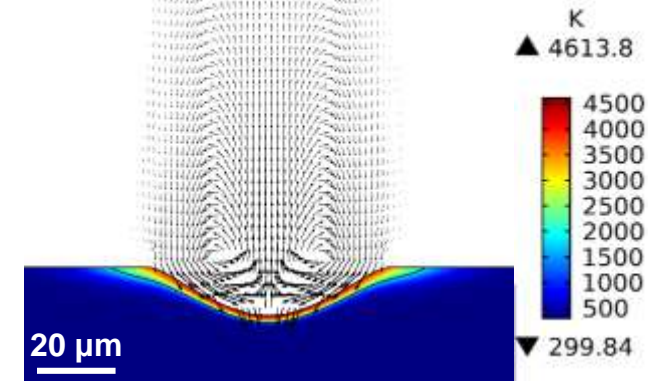
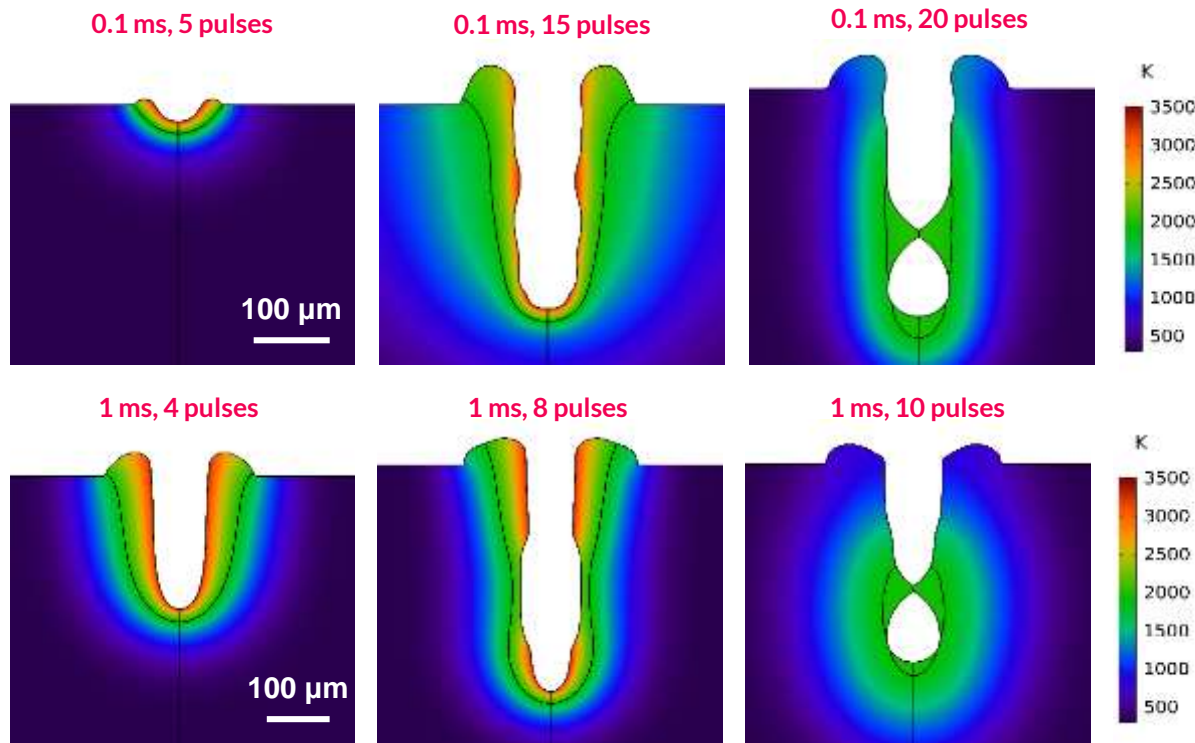
Numerical Simulation of Melt Hydrodynamics in Laser drilling

Laser power 200W
 Pulse width 1 ms
 Rep rate 10Hz
 Material: Ti
 Radius:- 100 μm



Numerical Simulation of Melt Hydrodynamics in Laser drilling

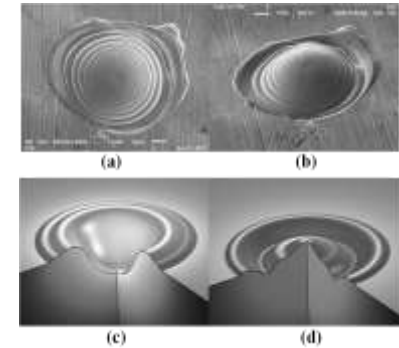
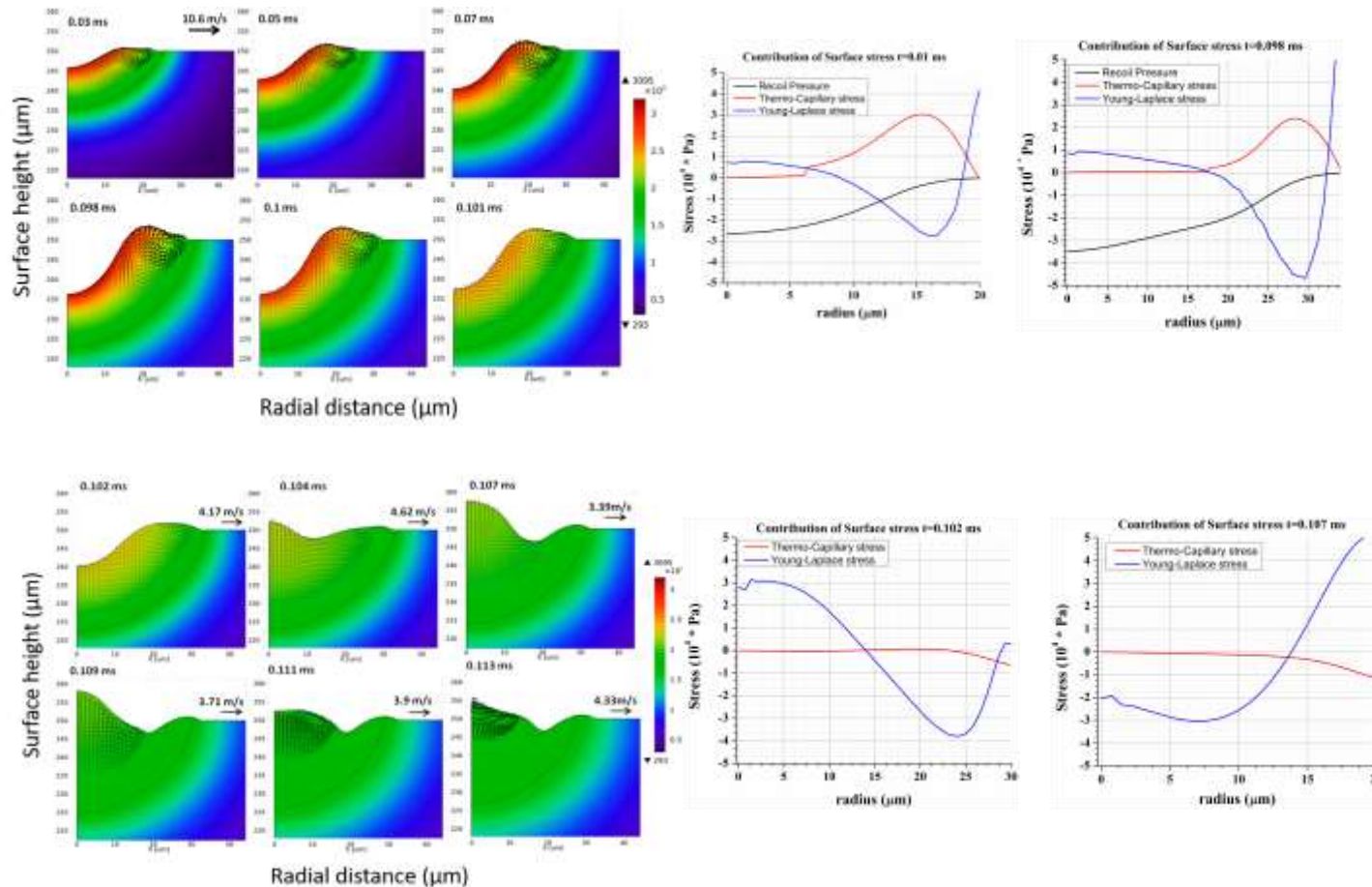
Role of Pulse Width



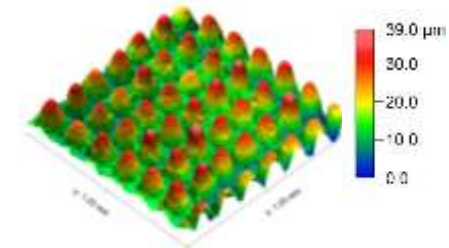
Transient melt pool dynamics in laser drilling, Fluence = $3\text{J}/\text{cm}^2$, at 20 ns irradiation time.

Laser Surface texturing: Micro hump conundrum

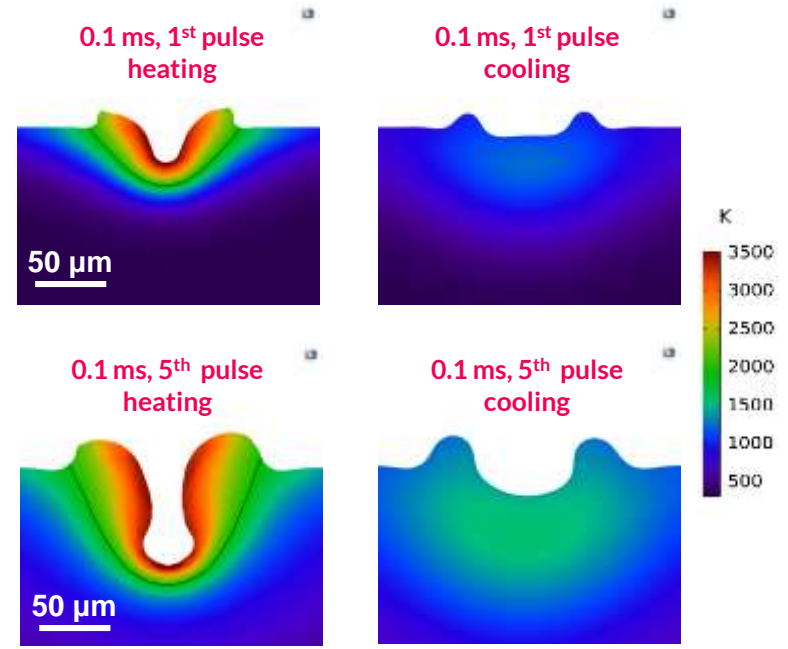
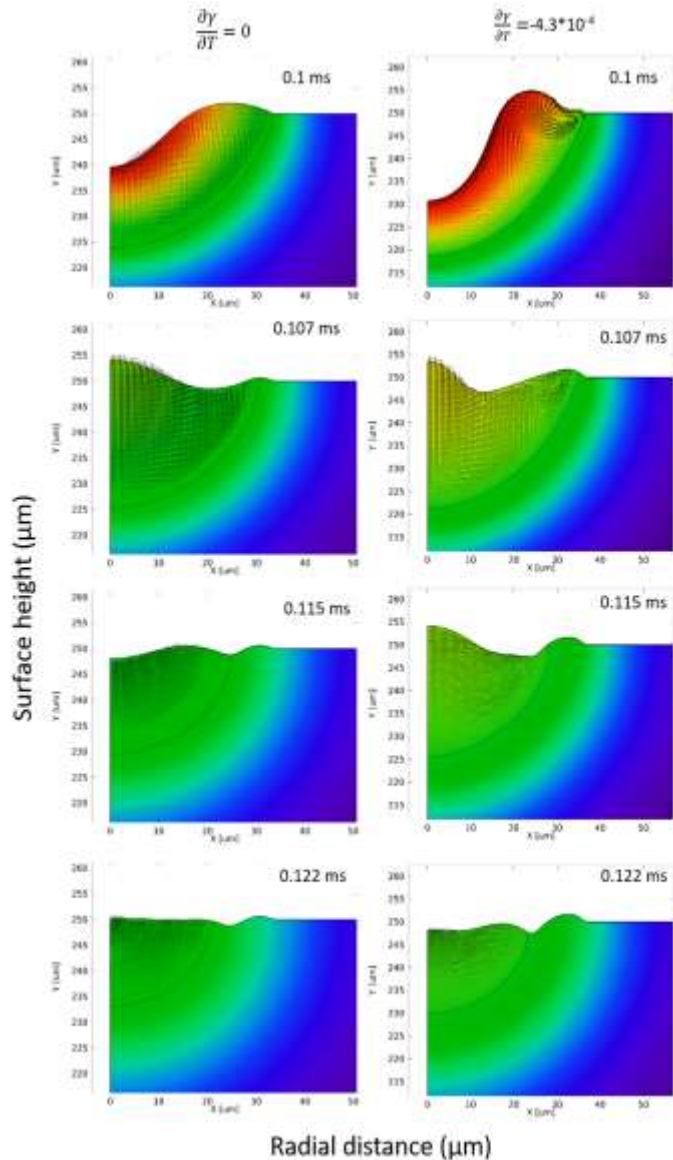
Transient Melt Pool Hydrodynamics



Qualitative comparison of surface topography for $P=70\text{W}$, $\text{dia}=73\mu\text{m}$. (a) SEM micrograph (top view) (b) SEM micrograph (tilted view) (c) 270° revolute profile of simulated melt geometry at $t=0.1$ ms (d) $t=0.4$ ms.

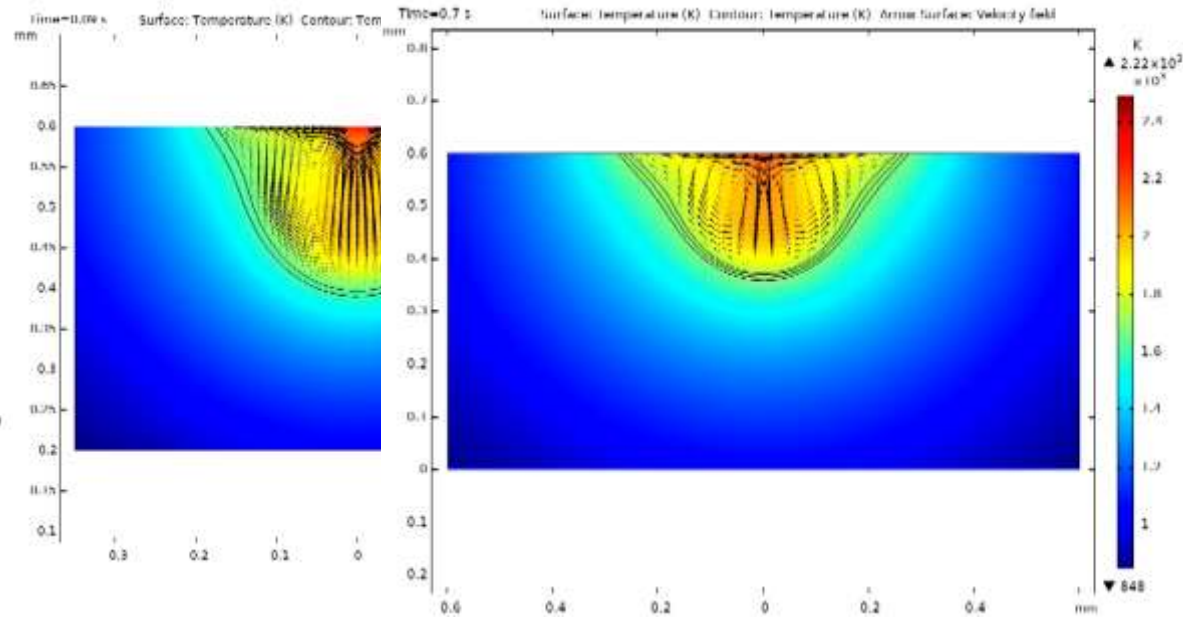
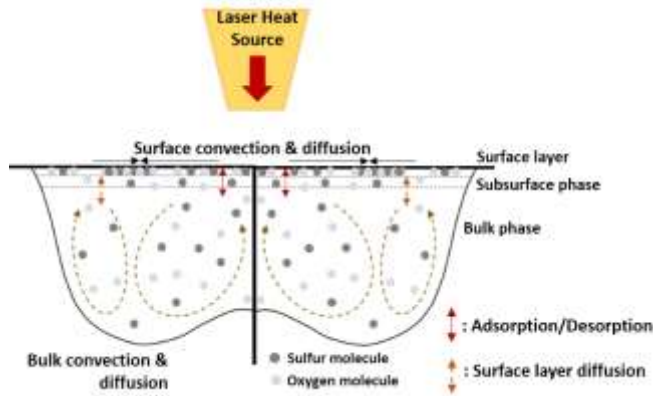


Laser Surface texturing: Bump to crater transition



$P = 100\text{W}, 0.1\text{ ms}, \text{Ti6AlV4}, \frac{\partial \gamma}{\partial T} = -2.8 \times 10^{-4} \text{ N}/(\text{m}^*\text{K})$

Melt Hydrodynamics in Conduction mode Laser welding



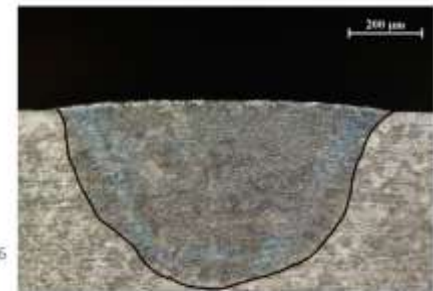
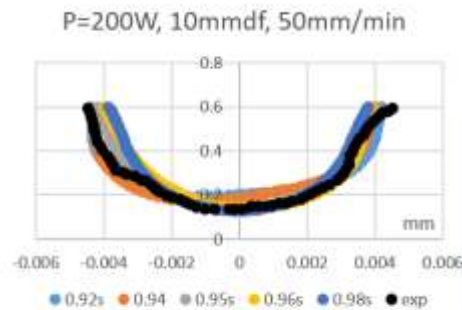
$$\frac{\partial C_i}{\partial t} + (\vec{u} \cdot \nabla) C_i = D_i \nabla^2 C_i$$

$$\frac{\partial \Gamma_i}{\partial t} + \nabla_s (\Gamma_i \vec{u}_s) = \nabla_s^2 \Gamma_i + S_i$$

$$S_i = \beta'_i C_{s,i} \left(\Gamma_{\infty,i} - \Gamma_i - \sum_j \Gamma_j \frac{\Gamma_{\infty,i}}{\Gamma_{\infty,j}} \right) - \alpha'_i \Gamma_i, \quad j \geq 2.$$

$$C_i = \frac{\alpha'_i}{\beta'_i} \left(\frac{\Gamma_i}{\Gamma_{\infty,i} - \Gamma_i - \sum_j \Gamma_j \frac{\Gamma_{\infty,i}}{\Gamma_{\infty,j}}} \right) \quad \alpha'_{i,var,cor} = C_i \mathcal{P}_i f_i$$

$$\left(\frac{\partial \sigma}{\partial T} \right)_{multi} = \sum_i -A_{\sigma,i} - RT \ln(1 + K'_{seg,i} a'_i) - \frac{K'_{seg,i} a'_i}{1 + K'_{seg,i} a'_i} \frac{\Gamma'_{\infty,i} \Delta H_i^0}{T}$$



(a)

(b)

Melt Hydrodynamics in Keyhole mode Laser micro welding

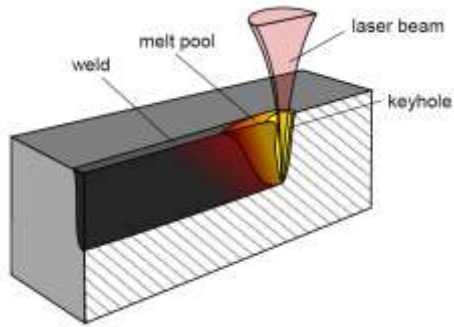
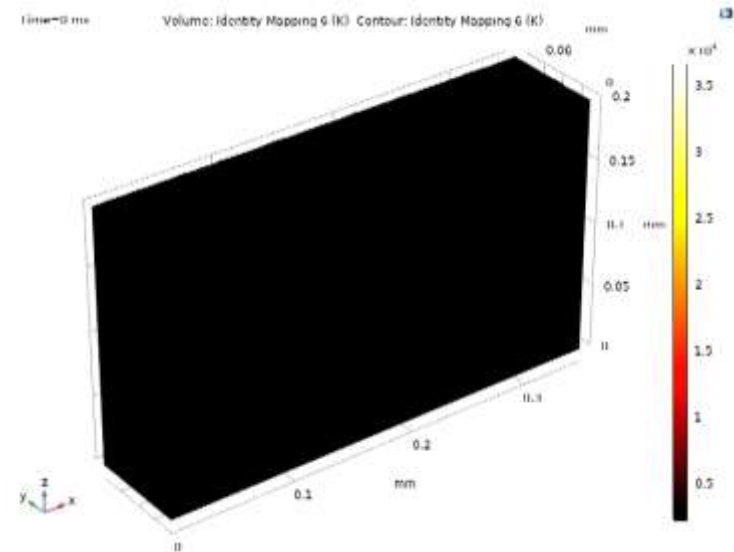
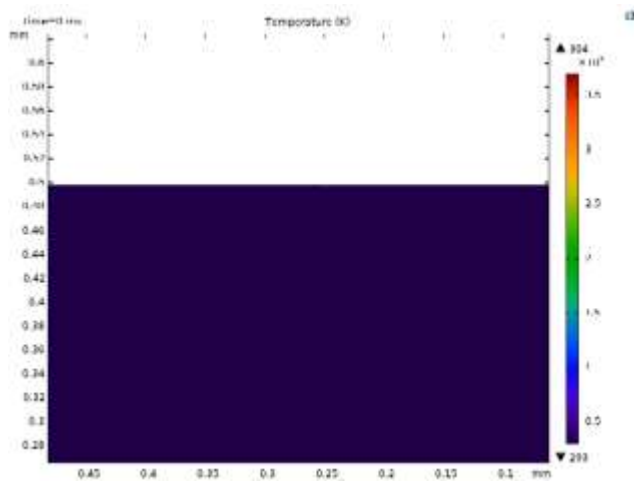
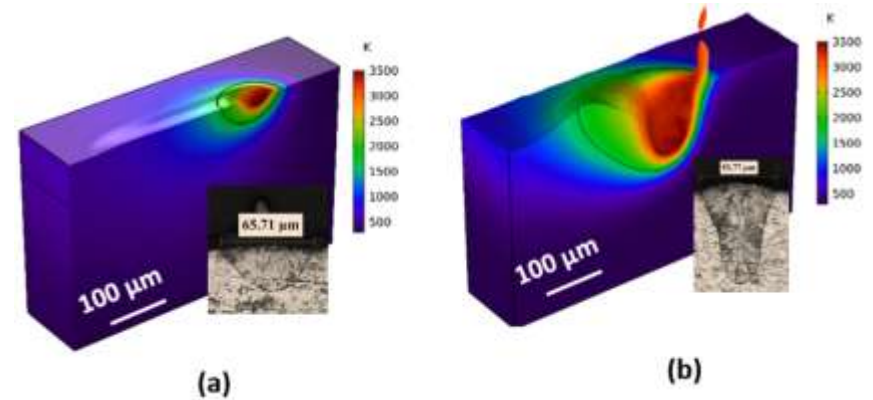
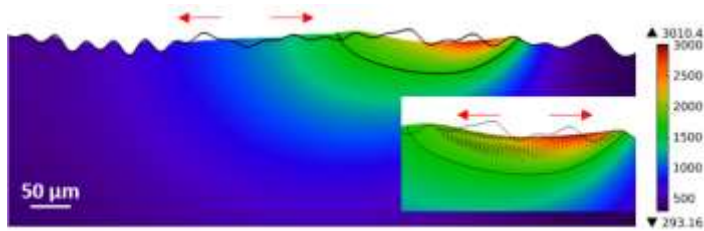
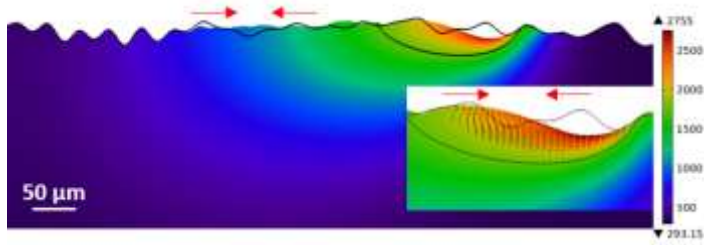


Image Source: http://www.ionix.fi/content/wp-content/uploads/2015/10/laser_welding.jpg



Melt Hydrodynamics in Laser polishing



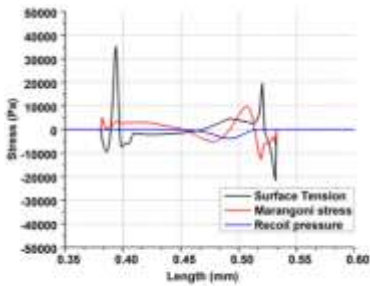
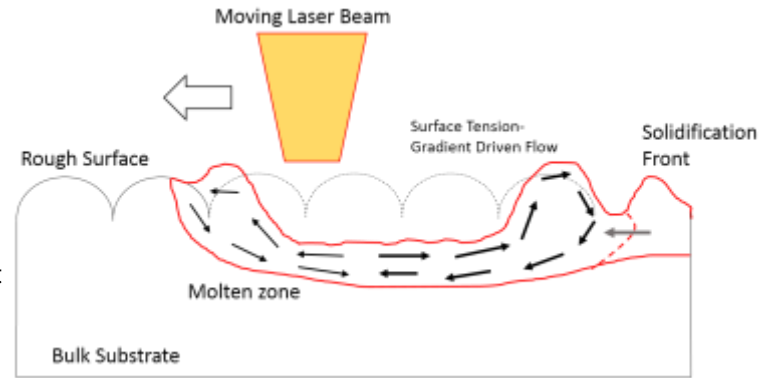
Shallow melting



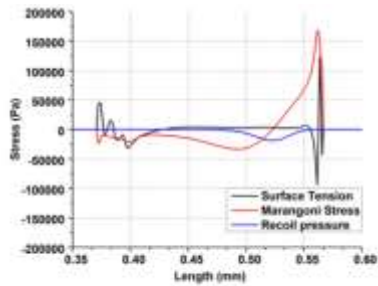
Surface Tension Gradient induced suppression



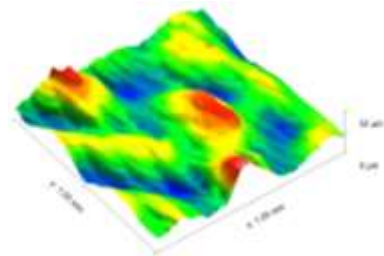
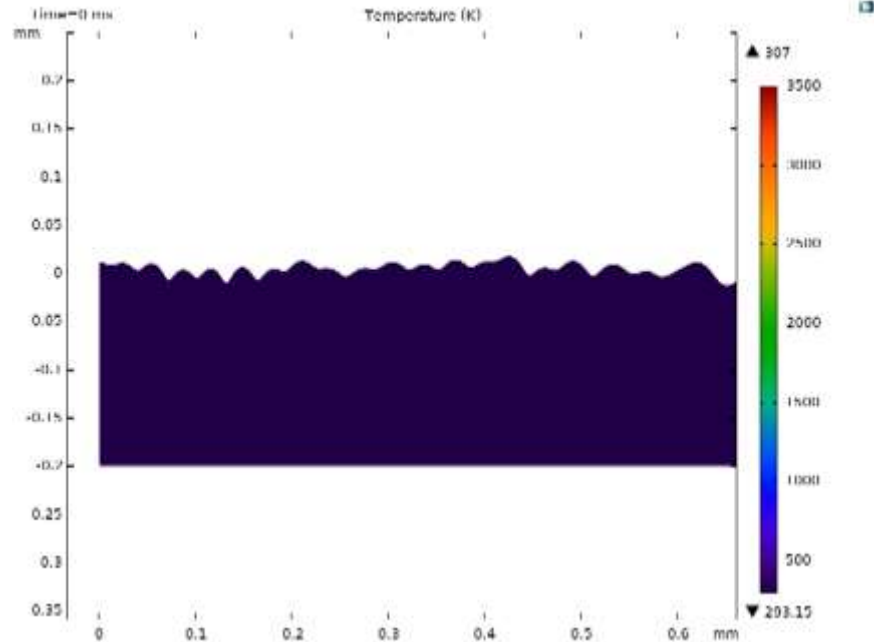
Surface Over Melting



(a)



(b)



Thanks!

Any questions?

Contact:

Shashank Sharma

Research Scholar

Laser Material Processing Lab

Dept. of Mechanical Engineering

IIT Kanpur

E-mail: kshashan@iitk.ac.in